

## Fabrication and optical properties of $C/\beta$ -SiC/Si hybrid rolled-up microtubes

G. S. Huang, Y. F. Mei, F. Cavallo, S. Baunack, E. Coric, T. Gemming, F. Bertram, J. Christen, R. K. Y. Fu, Paul K. Chu, and O. G. Schmidt

Citation: *Journal of Applied Physics* **105**, 016103 (2009); doi: 10.1063/1.3039089

View online: <https://doi.org/10.1063/1.3039089>

View Table of Contents: <http://aip.scitation.org/toc/jap/105/1>

Published by the *American Institute of Physics*

---

### Articles you may be interested in

[Optical properties of rolled-up tubular microcavities from shaped nanomembranes](#)

*Applied Physics Letters* **94**, 141901 (2009); 10.1063/1.3111813

[Tuning magnetic properties by roll-up of Au/Co/Au films into microtubes](#)

*Applied Physics Letters* **94**, 102510 (2009); 10.1063/1.3095831

[System investigation of a rolled-up metamaterial optical hyperlens structure](#)

*Applied Physics Letters* **95**, 083104 (2009); 10.1063/1.3211115

[Uniaxial and tensile strained germanium nanomembranes in rolled-up geometry by polarized Raman scattering spectroscopy](#)

*AIP Advances* **5**, 037115 (2015); 10.1063/1.4914916

[A unified model of drag force for bubble-propelled catalytic micro/nano-motors with different geometries in low Reynolds number flows](#)

*Journal of Applied Physics* **117**, 104308 (2015); 10.1063/1.4915114

[Three dimensional strain distribution of wrinkled silicon nanomembranes fabricated by rolling-transfer technique](#)

*Applied Physics Letters* **103**, 264102 (2013); 10.1063/1.4857875

---

Quantum Design Brings You the Next Generation Magneto-Optic Cryostat

Only be limited by your imagination...

Room Temperature Window  
Split-Coil Conical Magnet  
Sample Pod  
User Wiring Ports

Learn More

Quantum Design  
qdusa.com/opticool5

8 Optical Access Ports: 7 Side; 1 Top  
Temperature Range: 1.7 K to 350 K  
7 T Split-Coil Conical Magnet  
Low Vibration: <10 nm peak-to-peak  
89 mm x 84 mm Sample Volume  
Automated Temperature & Magnet Control  
Cryogen Free

## Fabrication and optical properties of C/ $\beta$ -SiC/Si hybrid rolled-up microtubes

G. S. Huang,<sup>1,a)</sup> Y. F. Mei,<sup>1,b)</sup> F. Cavallo,<sup>1</sup> S. Baunack,<sup>1</sup> E. Coric,<sup>1</sup> T. Gemming,<sup>2</sup>

F. Bertram,<sup>3</sup> J. Christen,<sup>3</sup> R. K. Y. Fu,<sup>4</sup> Paul K. Chu,<sup>4</sup> and O. G. Schmidt<sup>1</sup>

<sup>1</sup>*Institute for Integrative Nanosciences, IFW Dresden, Helmholtzstr. 20, D-01069 Dresden, Germany*

<sup>2</sup>*Institute for Complex Materials, IFW Dresden, Helmholtzstr. 20, D-01069 Dresden, Germany*

<sup>3</sup>*Fakultät für Naturwissenschaften, Institut für Experimentelle Physik, Otto-von-Guericke-Universität Magdeburg, Universitätsplatz 2, D-39106 Magdeburg, Germany*

<sup>4</sup>*Department of Physics and Materials Science, City University of Hong Kong, Tat Chee Avenue, Hong Kong, SAR, People's Republic of China*

(Received 8 September 2008; accepted 22 October 2008; published online 8 January 2009)

C/ $\beta$ -SiC/Si hybrid microtubes have been fabricated by releasing prestressed C/Si bilayer structures and treating with a postannealing process. Detailed characterization reveals the synthesis of  $\beta$ -SiC via a solid phase reaction at the C/Si interface. Remarkably, the production of  $\beta$ -SiC is promoted in the tube wall by rolled-up bonding of adjacent windings, which increases the area of the C/Si interface by a factor of 2. The Raman spectra acquired from the hybrid microtubes disclose peaks pertaining to the optical phonon modes of  $\beta$ -SiC that exhibit obvious downshifts due to surface effects on the SiC nanoparticles. Moreover, two light emission bands are detected from a hybrid microtube and their origin is discussed based on spectral analyses. © 2009 American Institute of Physics. [DOI: 10.1063/1.3039089]

In recent years, fabrication of rolled-up micro-/nano-objects<sup>1,2</sup> by releasing prestressed thin layers from substrates has attracted increasing interest due to promising applications in mechanics,<sup>3</sup> fluidics,<sup>4</sup> electronics,<sup>5</sup> optics,<sup>6</sup> as well as in several other interdisciplinary research fields.<sup>7</sup> This technique relies on self-organization and has been achieved in several materials systems.<sup>1-9</sup> In particular, rolling up multilayers on Si-on-insulator (SOI) substrates allows to integrate the rolled-up technology with mainstream Si planar technology, rendering it suitable for on-chip applications.<sup>10</sup> In our previous work, a SiGe layer was grown on top of a Si layer to create highly strained SiGe on insulator after a postoxidation/annealing process.<sup>10</sup> By using this approach, SiGe microtubes were fabricated but no chemical reaction between the two layers was reported (apart from interdiffusion). In another work, a focused laser beam was used to locally modify the tube wall by thermal treatment.<sup>11</sup> Herein, a diamondlike carbon (DLC) layer is deposited on an SOI substrate and serves both as a stressor as well as a reactant in the postannealing treatment after tube formation. C/ $\beta$ -SiC/Si hybrid microtubes are obtained via synthesis of  $\beta$ -SiC in a solid phase reaction at the C/Si interfaces. Since a multilayered tube wall is formed by rolling, additional C/Si interfaces are created, leading to a notable enhancement of SiC productivity. These hybrid microtubes may have advantages in microelectromechanical systems due to the outstanding physical and electronic properties of SiC.<sup>12,13</sup> For instance, it may be a suitable unit for electronic devices in high-temperature, high-power, and high-frequency applications.

The SOI wafer used in this experiment consists of a 27 nm Si (001) layer on a 100 nm SiO<sub>2</sub> film. A 20-nm-thick DLC layer was deposited using acetylene plasma [see Fig. 1(a)]. To prepare the rolled-up microtubes, the starting edge for the etching process was defined by a mechanical scratch along the  $\langle 010 \rangle$  direction.<sup>10</sup> The SiO<sub>2</sub> sacrificial layer was chemically removed by a 49% HF solution. The obtained microtubes were then subjected to postannealing in Ar. The morphology of the sample was investigated by using a combination of scanning electron microscopy (SEM) (in Zeiss NVision40 workstation) and transmission electron microscopy (TEM) (FEI Tecnai F30). Raman spectra were taken by a Renishaw inVia Raman microscope with a 325 nm HeCd laser as the light source. The low temperature cathodoluminescence (CL) measurement was performed in a home-made setup based on a modified JEOL 6400 SEM.

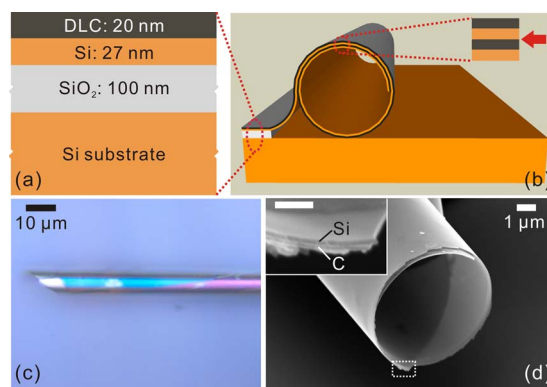


FIG. 1. (Color online) Schematic diagram of (a) as-grown structure containing a DLC layer and an SOI substrate and (b) rolled-up microtube after release of the prestressed DLC/Si bilayer. (c) Optical microscope image of a typical DLC/Si bilayered microtube. (d) SEM image of a microtube protruding from the substrate. The inset shows an enlarged image of the area marked by the dashed rectangle (scale bar: 200 nm).

<sup>a)</sup> Author to whom correspondence should be addressed. Electronic mail: g.huang@ifw-dresden.de.

<sup>b)</sup> Electronic mail: y.mei@ifw-dresden.de.

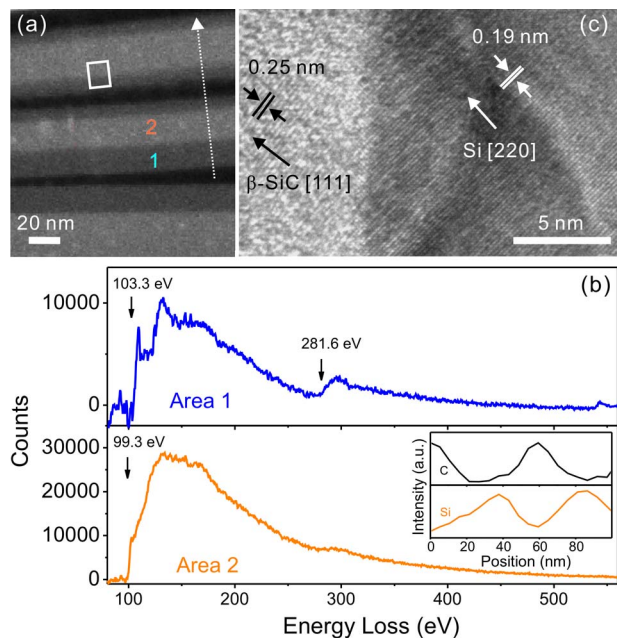


FIG. 2. (Color online) (a) Dark-field STEM image of the multilayered tube wall of a microtube annealed at 900 °C for 2 h. (b) EEL spectra collected from two different areas in (a). The inset shows the C and Si concentration profiles obtained by EELS analysis along the dashed arrow in (a). (c) HRTEM image of the region marked by the rectangle in (a).

Optical microscopy indicates that after being released, the free DLC/Si bilayer bends downward toward the substrate and eventually rolls up into a tubular structure, as depicted in Fig. 1(b). The typical optical image displayed in Fig. 1(c) shows that the microtube is straight and has a uniform diameter of  $\sim 7 \mu\text{m}$ . The coloration/contrast evolution along the microtube originates from the diffraction interference of light at different regions of the tube wall with different number of rotations.<sup>14</sup> Figure 1(d) shows an SEM image of a microtube protruding from the substrate. The image reveals a circular cross section of a microtube with one and a half rotations at the opening and a smooth inner/outer surface. The region marked by the dashed rectangle is enlarged in the inset of Fig. 1(d) in which the bilayer can be readily observed, along with the compact combination between the two layers remaining even after the roll-up process. Moreover, it should be mentioned that no rolled-up microtubes were obtained in the control sample without a DLC layer, implying that the DLC layer acts as a stressor in contact with the Si layer. Due to the bend-down behavior of the bilayer, we believe that the DLC layer should have an inherent compressive strain.<sup>15</sup> As soon as the bilayer is released, the DLC layer relaxes outwards, causing the bilayer to bend downwards.

Figure 2(a) shows the dark-field scanning TEM (STEM) image of the multilayered tube wall of a microtube annealed at 900 °C for 2 h. Here, *in situ* electron energy loss spectroscopy (EELS) is employed to perform a chemical analysis of the tube wall. According to the line scan results in the inset of Fig. 2(b), it can be concluded that the black and light gray (area 2) areas in Fig. 2(a) correspond to the C and Si layers, respectively. To clarify the composition of the dark gray interface region (area 1), an EELS spectrum is collected

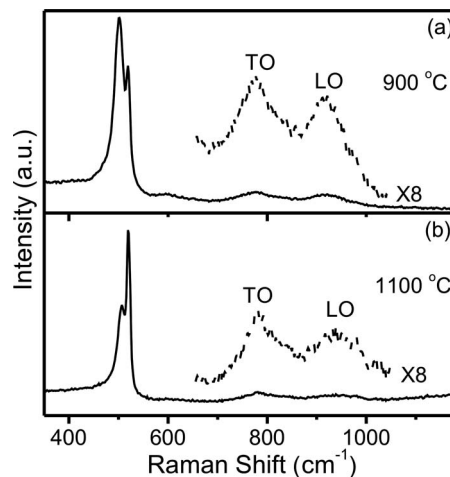


FIG. 3. Raman spectra of the hybrid microtubes annealed at (a) 900 and (b) 1100 °C.

and displayed in Fig. 2(b). The Si  $L_{3,2}$ -edge shifts to a higher energy at 103.3 eV (from 99.3 eV for pure Si) and the C  $K$ -edge shifts to a lower energy at 281.6 eV (from 284 eV for pure C), indicating a strong chemical bonding between Si and C.<sup>16,17</sup> The synthesis of SiC can be further corroborated by high resolution TEM (HRTEM) observation in the rectangular region of Fig. 2(a). The right part of the HRTEM image in Fig. 2(c) exhibits parallel lattice fringes with a distance of 0.19 nm, indicating a crystal orientation of [220] in the Si layer. In comparison, in the left part (i.e., area 1), lattice fringes in a nanoparticle are observed and the fringe distance (0.25 nm) is the same as the spacing of the {111} planes of  $\beta$ -SiC.<sup>17</sup> It should be stressed that in our experiments, SiC is produced via a solid phase chemical reaction that takes place at the C/Si interface during annealing, and therefore, the fact that we can detect SiC nanoparticles with a size of 3–5 nm in the dark gray interface layer located at both sides of the Si layer illustrates the synthesis of SiC at the additional C/Si interface produced by rolled-up bonding [see the red arrow in Fig. 1(b)]. In addition, the existence of  $\text{SiO}_x$  can be verified by Auger electron spectroscopy (not shown here) and the observation of oxygen in area 1 [see the weak O  $K$  edge at 535.4 eV in the upper spectrum of Fig. 2(b)]. We suggest that the oxygen in the oxides may come from the residual oxygen in the furnace and/or the top native oxide layer of the Si layer in SOI.

Figures 3(a) and 3(b) display the Raman spectra of hybrid microtubes annealed at 900 and 1100 °C, respectively. Two broad peaks centered at 776 and 921  $\text{cm}^{-1}$  can be seen from the sample annealed at 900 °C [Fig. 3(a)], whereas they shift to 783 and 941  $\text{cm}^{-1}$ , respectively, in the sample annealed at 1100 °C [Fig. 3(b)]. According to previous investigations of Raman properties of  $\beta$ -SiC,<sup>18,19</sup> the low-wavenumber peak can be assigned to the zone-edge TO phonon and the other to the LO mode. It is worth noting that the two optical phonon modes in both samples exhibit obvious downshifts compared to those in bulk  $\beta$ -SiC, especially in the sample annealed at 900 °C. The decrease in the phonon frequencies in the  $\beta$ -SiC nanoparticles are considered to be related to the phonon confinement effect in SiC

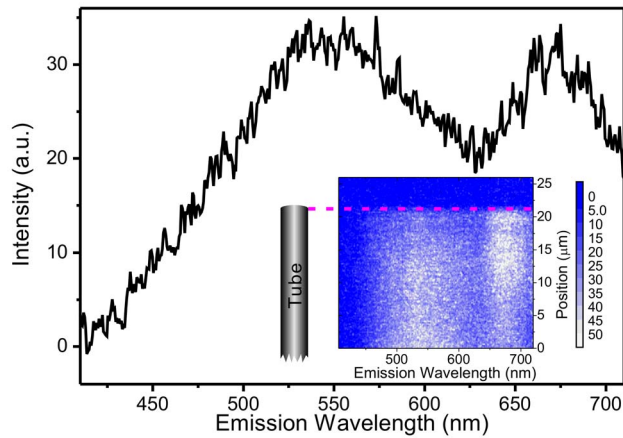


FIG. 4. (Color online) CL spectrum of a hybrid microtube annealed at 900 °C. The inset shows a series of CL spectra collected along the tube axis.

nanoparticles<sup>20</sup> and the lattice imperfection near the surface, which is more prominent in the LO mode.<sup>18</sup> In the sample annealed at lower temperature, the nanoparticles are smaller, and the stronger influence from the surface should lead to significant downshifts of the optical phonon modes. On the other hand, for the sample annealed at higher temperature, the Raman peaks exhibit a smaller downshift due to larger particle size, as displayed in Fig. 3(b). Another notable feature in the Raman spectra is the splitting of the TO mode of Si. The sharper peak at 520  $\text{cm}^{-1}$  originates from the Si substrate while the broader peak at smaller wavenumbers originates from the tensile strained Si layer in the tube wall. The average stress ( $\varepsilon$ ) can be estimated using the following equation:  $\varepsilon = 250 \times \Delta\omega$  (MPa),<sup>21</sup> where  $\Delta\omega$  is the shift of the TO mode with respect to the Si substrate. The average tensile stresses of the Si layers in the microtubes annealed at 900 and 1100 °C are 4.5 and 3.3 GPa, respectively. The reduction in tensile stress reflects the relaxation of strain and the change in the microstructure in the sample annealed at higher temperature. In addition, the broadening of the TO mode compared to the bulk Si can be attributed to the nanometer size of the tube wall and a pronounced strain gradient in the Si layer.<sup>22</sup>

Light emission properties of SiC continue to be a focus of many investigations.<sup>23,24</sup> Here, we also measure the CL spectra of the hybrid microtube at 5 K and the results are shown in Fig. 4. Judged from the spectral position, the high-energy band at  $\sim 550$  nm (2.25 eV) could be assigned to the band-to-band recombination in the  $\beta$ -SiC nanoparticles. The broadening of this emission band can be attributed to the variation in particle size,<sup>23</sup> which further supports our interpretation, although we cannot completely rule out the possibility of this emission being connected with defect centers. However, the low-energy band at  $\sim 670$  nm (1.85 eV) should have another origin. Previous experimental investigations have disclosed a defect center named as nonbridging oxygen hole center (NBOHC) in silicon oxide for the emission at 1.85 eV.<sup>25,26</sup> Considering the similar emission energy

and microstructure, we believe that the low-energy CL band in the hybrid microtube may originate from the optical transition in NBOHC. For verification, we collect a series of CL spectra along the tube axis (see inset of Fig. 4). The enhancement of a low-energy band at the region near the opening of the microtube, where more  $\text{SiO}_x$  exists due to the excess oxidation of residual oxygen, is observed. This phenomenon supports the conclusion that the low-energy CL band is connected with NBOHC in  $\text{SiO}_x$ . The inset of Fig. 4 also indicates the competition between the synthesis of SiC and  $\text{SiO}_x$ : the high-energy and the low-energy bands exhibit opposite tendencies in the intensity evolution along the tube axis.

In summary, we have fabricated C/ $\beta$ -SiC/Si hybrid microtubes by releasing prestressed DLC/Si bilayers from SOI substrates followed by a postannealing treatment. During annealing,  $\beta$ -SiC is synthesized via a solid phase reaction at the C/Si interface. The roll-up process provides the advantage of increasing the C/Si interface area via rolled-up bonding, thereby promoting the production of SiC. Obvious downshifts of two optical phonon modes of  $\beta$ -SiC can be observed in the Raman spectra and are attributed to the surface effect. In addition, CL spectra exhibit two emission bands from the microtubes. Spectral analyses indicate that they may originate from band-to-band recombination in  $\beta$ -SiC and optical transition in NBOHC, respectively.

We are grateful for the help of Dr. Christoph Deneke, Jochen Werner, Elliot John Smith, Dr. Wolf-Dieter Wagner, Dominic J. Thurmer, and Dr. Juliane Gabel. Financial support by the BMBF (Contract No. 03X5518) and Hong Kong Research Grants Council (RGC) General Research Funds (GRF) Grant No. CityU 112307 are acknowledged.

<sup>1</sup>V. Ya. Prinz *et al.*, *Physica E* **6**, 828 (2000).

<sup>2</sup>O. G. Schmidt and K. Eberl, *Nature (London)* **410**, 168 (2001).

<sup>3</sup>L. Zhang *et al.*, *Nano Lett.* **6**, 1311 (2006).

<sup>4</sup>D. J. Thurmer *et al.*, *Appl. Phys. Lett.* **89**, 223507 (2006).

<sup>5</sup>O. G. Schmidt *et al.*, *IEEE J. Sel. Top. Quantum Electron.* **8**, 1025 (2002).

<sup>6</sup>R. Songmuang *et al.*, *Appl. Phys. Lett.* **90**, 091905 (2007).

<sup>7</sup>Y. F. Mei *et al.*, *Adv. Mater. (Weinheim, Ger.)* **20**, 4085 (2008).

<sup>8</sup>O. Schumacher *et al.*, *Appl. Phys. Lett.* **86**, 143109 (2005).

<sup>9</sup>L. Zhang *et al.*, *Appl. Phys. Lett.* **92**, 143110 (2008).

<sup>10</sup>F. Cavallo *et al.*, *Appl. Phys. Lett.* **90**, 193120 (2007).

<sup>11</sup>C. Deneke *et al.*, *Appl. Phys. Lett.* **84**, 4475 (2004).

<sup>12</sup>S. G. Sundaresan *et al.*, *Chem. Mater.* **19**, 5531 (2007).

<sup>13</sup>M. W. Zhao *et al.*, *Phys. Rev. B* **71**, 085312 (2005).

<sup>14</sup>K. S. Novoselov *et al.*, *Science* **306**, 666 (2004).

<sup>15</sup>E. Liu *et al.*, *J. Appl. Phys.* **98**, 073515 (2005).

<sup>16</sup>X. H. Sun *et al.*, *J. Am. Chem. Soc.* **124**, 14464 (2002).

<sup>17</sup>T. Seeger *et al.*, *Adv. Mater. (Weinheim, Ger.)* **12**, 279 (2000).

<sup>18</sup>Y. Sasaki *et al.*, *Phys. Rev. B* **40**, 1762 (1989).

<sup>19</sup>Y. Ward *et al.*, *J. Appl. Phys.* **102**, 023512 (2007).

<sup>20</sup>A. Colli *et al.*, *Nano Lett.* **8**, 2188 (2008).

<sup>21</sup>I. De Wolf, *Semicond. Sci. Technol.* **11**, 139 (1996).

<sup>22</sup>R. Songmuang *et al.*, *Appl. Phys. Lett.* **88**, 021913 (2006).

<sup>23</sup>X. L. Wu *et al.*, *Phys. Rev. Lett.* **94**, 026102 (2005) (and references therein).

<sup>24</sup>J. Y. Fan *et al.*, *Prog. Mater. Sci.* **51**, 983 (2006).

<sup>25</sup>D. L. Griscom, *J. Non-Cryst. Solids* **73**, 51 (1985).

<sup>26</sup>M. A. S. Kalceff and M. R. Phillips, *Phys. Rev. B* **52**, 3122 (1995).